Advanced Technologies in Water Efficiency
homepage:https://atwe.razi.ac.ir
Online ISSN:2783-4964

The effect of vortex on head loss and pressure fluctuation along the Penstock of Hydroelectric power plant

Reza Roshan [1], and **Rasool Ghobadian** [2]✉

1. Department of Water Engineering, Razi University, Kermanshah, Iran. E-mail: rezaroshan2631@gmail.com,
2. Corresponding author, Department of Water Engineering, Razi University, Kermanshah, Iran. E-mail: r_ghobadian@Razi.ac.ir

Article Info

Article type:
Research Article

Article history:
Received 30 July 2025
Received in revised form 14 October 2025
Accepted 18 November 2025
Available online 22 December 2025

Keywords:
physical model,
vortex,
pressure fluctuations,
anti-vortex plate,
hydroelectric power plant,
penstock.

ABSTRACT

Objective: This study aimed to assess the hydraulic impacts of intake vortices on energy losses and pressure fluctuations in hydropower penstocks and to evaluate the effectiveness of horizontal perforated anti-vortex plates in mitigating these effects.

Method: A large-scale laboratory model was used to systematically examine the influence of intake vortices under a wide range of hydraulic conditions. The experiments were conducted by varying the relative submergence depth (S/D = 1.5, 1.75, 2.0, 2.5, and 3.0) and the intake Froude number (Fr = 0.6, 0.8, 1.0, and 1.2) to generate different vortex strengths. Hydraulic parameters, including relative total head loss, relative friction head loss, Darcy–Weisbach friction coefficient, and pressure fluctuations, were measured along the penstock. Pressure fluctuations were recorded at nine measurement sections distributed along the penstock, and the hydraulic performance was compared for cases with and without the installation of an anti-vortex plate.

Results: The experimental results clearly demonstrated that the installation of an anti-vortex plate significantly reduced hydraulic losses and pressure fluctuations. On average, the friction coefficient, relative total head loss, and relative friction head loss were reduced to approximately 19.2%, 44.4%, and 20.8% of their corresponding values without the plate, respectively. Increasing the submergence ratio led to a notable increase in relative friction head loss, while the friction coefficient decreased. For a fixed submergence depth, higher Froude numbers intensified vortex strength, resulting in increased total and friction head losses as well as more pronounced pressure fluctuations along the penstock, despite a reduction in the friction coefficient. The dissipation length of vortices was found to depend strongly on vortex class, with weak Class C vortices dissipating within approximately 7 diameters from the intake, Class B vortices persisting up to about 18 diameters, and strong Class A vortices showing no clear dissipation within the tested penstock length.

Conclusions: Intake vortices have a substantial adverse effect on the hydraulic performance of hydropower penstocks by increasing energy losses and inducing pressure fluctuations. The results confirm that horizontal perforated anti-vortex plates are an effective and practical solution for mitigating vortex-induced losses and stabilizing flow conditions at intakes. Furthermore, the findings highlight the critical role of submergence depth and intake Froude number in controlling vortex strength and persistence. For strong air-core vortices, considerably longer penstocks or additional mitigation measures may be required to ensure complete vortex attenuation, underscoring the importance of vortex control in the design and operation of hydropower intakes.

Cite this article: Sabetimani, A., Amer., Sajjadi, S.M., Fathi Moghadam, M., Keramat, A., & Ahadiyan, J. (2025). Investigating fluid-structure interaction and transient flow dynamics for enhanced pipeline fault detection. *Advanced Technologies in Water Efficiency, 5* (4), 108-128. https://doi.org/10.22126/atwe.2025.12399.1175

Publisher: Razi University.
https://doi.org/10.22126/atwe.2025.12399.1175

Introduction

Free surface vortices are a common and at the same time limiting phenomenon in all types of industrial intakes and their related hydro mechanical facilities. The formation of strong vortices in all types of intakes, including power plant intakes, is considered as an undesirable phenomenon. Especially in the situation where the vortex causes the entry of air and strong swirling flows into the water intake tunnel (Penstock). The occurrence of this phenomenon will cause severe drops in water intake efficiency, mechanical damages such as intensification of vibrations, corrosion and cavitation, as well as operational problems (Suerich-Gulick et al., 2014; Möller et al., 2012). Considering the importance of this issue, the amount of air influence into the intake caused by air-core vortices during detailed laboratory studies in recent years have been investigated (Keller et al., 2014 ; Möller et al, 2015). In hydroelectric power plants, at levels lower than the acceptable level, due to the formation of a vortex with the air core and the entry of air into the Penstock, the production of electrical energy faced a serious problem (Amiri et al., 2011). The history of research on the vortex goes back many years ago. In this relation, Rahm published a relatively complete set of records of theoretical studies before 1950 in a report, in which, in addition to describing the mechanism of formation of strong vortices, there are evidences of the decrease in intake efficiency due to the occurrence of strong vortices with air core(Rahm, 1953). Researchers believe that the formation of strong vortices at the water intakes imposes adverse effects on the structure of the water intakes and their adjacent facilities. The vortices formed on the surface of the water physically divided into six types (levels), from 1 to 6, as the level of the vortex increases; its strength also increases (Knauss, 1987). In terms of importance and degree of risk, the six types of vortex classified into three classes A, B and C (Sarkardeh et al., 2010). The relationship between these two types of classification with the physical characteristics of the vortex is shown in Fig. 1.

According to Fig. 1, class A includes vortices through which air enters the intake, so they are at the highest level in terms of importance and degree of risk. On the other hand, class C vortices mainly have surface rotations and have the lowest degree of risk. Class B vortices are also important because they cause the transfer of floating particles into the intake tunnel. In understanding the vortex and the factors affecting it, the contribution of laboratory studies and experimental models is more than other methods. Mechanism of vortex formation was studied by laboratory tests(Gulliver & Rindles, 1987). Using an experimental method, Sarkardeh et al. investigated the effect of the geometric and hydraulic conditions of the intake and reservoir on the strength of the vortices formed at a horizontal intake(Sarkardeh et al., 2012 ; Sarkardeh et al., 2013) . Azarpira et al. also investigated the flow conditions in the reservoir in the presence of a vortex using the laboratory model of the Karun III dam (Azarpira et al., 2014).

The most important design indicator of water intakes is critical submergence depth (Sc). The critical submergence depth is a water level at which the created air core is on the threshold of entering the intake (Fig. 2). As long as the submergence depth of the reservoir (Si) is greater than the critical submergence depth(Sc), air core can not enter the intake. On the contrary, in the condition that Si moves towards Sci and is less than Sc, a permanent and continuous air core is formed and enters the the intake. Due to the variety of factors affecting the vortex formation, the exact determination of the critical submergence depth is associated with complications (Knauss, 1987), in such a way that the general relationships presented in this field are empirical. Therefore, it is still necessary that the vortex phenomenon and the factors affecting the critical submergence depth is further studied and analyzed. In recent years, with the advancement of computer models, numerical methods have also been used in the study of the vortex phenomenon. As an example, we can refer to the study on the vortex flow created in a cylindrical tank containing a viscous fluid in steady state by direct numerical simulation

method. In this study, it was observed that there is a direct relationship between the parameters of the flow inside the tank and in the intake conduit, so that with the increase in the fluid rotation in the tank, the flow rotation inside the intake conduit also increases (Constantinescu & Patel, 1998). Partovi Azar et al.(2010), indicated that the critical submergence would depend on hydraulic conditions in intake structure and using FLUENT model, they showed that the most severe vortex created on the gates of Aydoghmush Dam's intake tower is type 3.

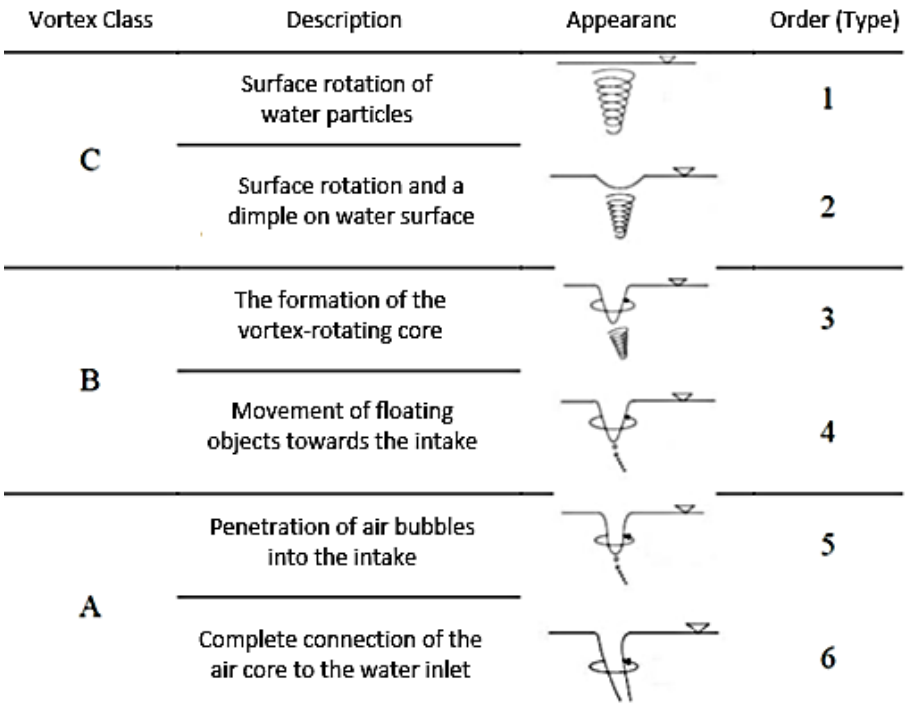

Figure 1. Vortex type visual classification (Sarkardeh et al. 2010)

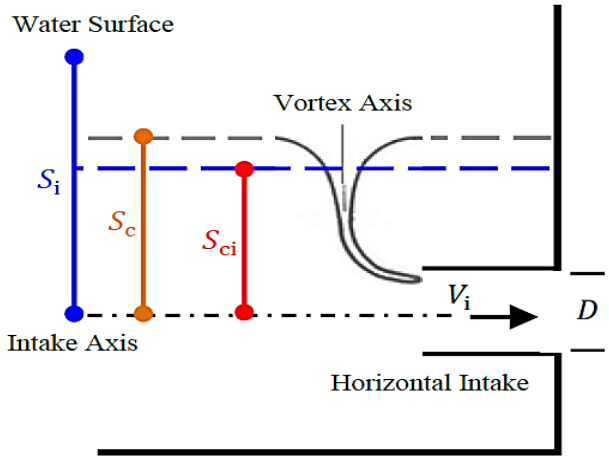

Figure 2. Critical submergence at a horizontal intake (Knauss, 1987)

Chelebioglu conducted a study on the friction coefficient and roughness changes in the Penstock of the power plant (ÇELEBIOĞLU, 2019). He noticed that when highly calcined water was passed through the Penstock of a hydroelectric plant, it left a residue on the surface of the pipe. The accumulated debris over time change pipe roughness and friction loss in the system and as a result, the head and flow rate on the turbine. He finally concluded that the surface roughness value (ε) equivalent to 0.3 mm could be used for calcined surfaces, which is much higher than steel surfaces but smaller than concrete. Sukhapure et al. conducted a research on head losses and prediction of these losses in two-branch penstocks (Y-Branch) with angles of 30°, 45°, 60° and 90°. Using Computational Fluid Dynamics (CFD) and simulation of branching, they presented a digital reference for head loss calculations for bifurcated penstocks (Sukhapure, 2018). In a research, Moukam et al. used the Colebrook-White equation to evaluate the turbulent boundary layer and friction along the penstock of the Three Gorges Dam, and concluded with 3D simulation in Fluent software that the slope of the penstock pipe has a significant effect on the development of the boundary layer and friction (Moukam et al., 2022). Roshan and Ghobadian studied effect of anti-vortex plates on vortex dissipation, discharge coefficient and inlet loss coefficient in hydropower intakes. Their results showed that the intake discharge coefficient reduces 5.9%, 10.5%, and 13.4% by using of perforated anti-vortex plate with openings of 70%, 58% and 50% respectively. It is also caused 12.9%, 24.7% and 33.5% for inlet loss coefficient of the intake, respectively (Roshan and Ghobadian, 2022). Aghajani et al. using image processing method and hydraulic PTV technique, investigated the flow through the horizontal intake with a trashrack. Their results showed that the best performance of the trashrack in reducing the vortex power occurred at the Froude number of one and on average, about 56% of the vortex power was reduced (Agbayani, et al., 2019). Manogaran et al. investigated the effect of two types of anti-vortex plates in mitigation of free-surface vortices in the dam intake using numerical simulation. Their results showed that square plates can be more effective in mitigation the free-surface vortices flow and decay of the vortex class than wedge edge plates (Manogaran et al., 2023). Zheng et al., in a review research work, systematically presented the hydrodynamic characteristics of the gravity surface vortex, including the mechanisms of evolution of flow pattern and the vibrations caused by the vortex. They also examined the future research directions in this matter (Zheng et al., 2023). Roshan and Ghobadian by physical model investigated the effect of reservoir geometric asymmetry, presence of unevenness in the bottom of the reservoir and angle of approach flow on the critical submergence depth (Roshan & Ghobadian, 2023).

A review of previous studies shows that research on power-plant penstocks generally focuses on various design methods aimed at minimizing construction and operating costs (e.g., Singhal & Kumar, 2015), reducing water consumption for hydropower generation (e.g., Leon, 2016), and optimizing geometric parameters of penstocks to increase the efficiency of gravity-fed power plants (e.g., Bajracharya et al., 2020). Although valuable achievements have been collected in these fields, however no specific research has been conducted to investigate the effect of vortex on the head loss and friction coefficient of Penstock of the power plant, as well as the analysis of pressure fluctuations along it in the presence of different type of vortexes. Considering the complexity of the subject and its importance, the conclusion of this findings require further research in this field. Therefore, in this research, using a large-scale laboratory model, the effect of vortex with different classes on energy loss along the horizontal water carrying tunnel (similar to Penstocks in hydroelectric power plants) has been investigated.

Method

Dimensional analysis

A review of previous research shows no formula has been provided to calculate the energy loss in the water carrying tunnel under the conditions of vortex entry with and without air core. The relationship between the parameters affecting the amount of head loss(h_f) in the Penstock can be introduced as follows:

$$h_f=f(D,V,S,g,\rho,\upsilon,\sigma,\Gamma,\varphi,L,\varepsilon) \quad (1)$$

Where inside diameter of the Penstock is D, volumetric mass of water is ρ , V is average velocity of flow in the Penstock, ν is kinematic viscosity of the fluid, gravitational acceleration is g, surface tension of the fluid is σ, Γ indicates circulation of vortex , angle of the approach flow is φ, submergence depth is S, L is the length of the tunnel and ε signifies the roughness of the tunnel.

by using dimensional analysis and integrating some dimensionless groups with each other, the following relationship is finally obtained to calculate the relative friction loss in the water carrying tunnel in the presence of the entrance vortex:

$$\frac{h_f}{L}=f(\frac{S}{D},Fr,Re,We,N_\Gamma,\frac{\varepsilon}{D},\varphi) \quad (2)$$

where the dimensionless groups in the right side of the relation are relative submergence depth of the intake (S/D), Froude number($V/\sqrt{gD}$), Reynolds number (VD/υ), Weber number($\rho V^2 D/\sigma$), circulation number(Γ/VD), relative roughness and angle of the approach flow, respectively.

Typically, Froude number similarity is used in vortex modeling where gravity and inertial forces have significant effects. However, there are effects of viscosity and surface tension, although their amount is small and they should be minimized. These limitations can be considered as criteria for determining the scale of the model. Various researchers have studied the scale effects in vortex physical model and have proposed minimum values for the Reynolds and Weber numbers to prevent scale effects caused by viscosity and surface tension of the fluid. Minimum values of Re≥7.7× 104 and We>600 (Padmanabhan and Larsen, 2001); and We>120 (Jain et al. 1978); Re≥5× 104 (Daggett and Keulegan, 1974) and Re≥1.1× 105 and We>720 (Odgaard, 1986) should be considered in the construction of the model. The minimum values of Reynolds and Weber numbers in this study are 1.2×10^5 and 1.2×10^3, respectively, which are higher than the minimum criteria provided to eliminate the effects of viscosity and surface tension. On the other hand in the experiments conducted in the current research, parameters φ, L, ε and D were considered constant. Additionally, the experiments conducted in (Roshan, 2023) showed that NΓ is a function of the submergence depth and the Froude number($N_\Gamma = 0.36\ (S/D)^{-0.69} Fr^{0.184}$). According to these explanations, in this study only the effect of two parameters, submergence depth (S/D) and Froude number($V/\sqrt{gD}$), on energy loss as well as pressure fluctioation along the Penstock and friction coeeficient have been investigated.

Laboratory model

Considering that the aim of this research is to investigate the effect of vortex with an air core (vortex of class A) and without air core on the longitudinal head loss of the penstock, the laboratory model should be able to create and develop the vortex of type 6 and different submergence depths (S/D). Achieving this requires that flow with different Froude numbers (Fr) can be generated for a fixed depth inside the water intake tunnel. Obviously, such an issue cannot be achieved in the case of gravity flow, because in gravity flow, the depth of water in the reservoir and the flow velocity (or Froude number) are directly related to each other. To

solve this problem in the model, a pump was directly connected to the end of water intake tunnel. By adjusting the speed of the pump electromotor, flow velocity can be adjusted independently of the water depth in the reservoir. In addition, to keep the water depth of the tank constant, at different flow rates, the return pipe was directed to the model tank, so there is always a constant amount of water circulating in the system. In this way, it is possible to fill the tank with water to a certain depth at the beginning and then by changing the speed of the electromotor, different discharges and as a result different Froude numbers can be created in the Penstock. The main components of the laboratory model are reservoir, water-carrying pipe (Penstock), pump and a device to control electromotor rotation, which are shown in Fig. 3. The model reservoir is 1.3 m wide, 3.5 m long and 2 m high. The intake projected 0.15 meters into the reservoir and placed in such a way that the walls and the bottom of the reservoir do not affect the flow conditions on it. The reason for the projecting of the intake into the reservoir is to simulate the dead zone of flow area above the water intake. The length of the penstock pipe is 4.5 meters and its inside diameter is 0.16 meters. At 2 meters upstream of the intake in the reservoir, there are vertical blades that can change the angle of the incoming flow towards the intake. This makes it possible to strengthen the upstream circulation to reach stronger vortices. This model was made in the Water Research Institute of the Ministry of Energy. Since in all conditions of the experiments, the Reynolds number was much more than 2000 (Table 1), the prevailing flow can be considered turbulent and independent of the Reynolds number. To eliminate the vortex, horizontal perforated plates were used on the forehead of the intake (Fig. 4).

Table 1. Geometric characteristics of the model and hydraulic parameters of the flow

Specifications	Parameters	Signs & Measure Units	Variation Range
Hydraulic	Flow Discharge	Q (m^3/s)	$0.015 \le Q \le 0.030$
	Flow Velocity	V (m/s)	$0.75 \le V \le 1.5$
	Submergence Depth	H or S (m)	$0.24 \le S \le 0.40$
	Froude Number	F_r	$0.60 \le F_r \le 1.19$
	Reynolds Number	R_e	$120000 \le R_e \le 240000$
	Relative submergence	S/D	$1.5 \le S/D \le 3.0$
Geometric	Anti-Vortex Plate Length	L (m)	$0.24 \le L \le 0.32$
	Anti-Vortex Plate Width	W (m)	$0.16 \le W \le 0.24$
	Reservoir Height	H_R (m)	2.0
	Penstock Diameter	D (m)	0.16
	Anti-Vortex Plate Thickness	T (m)	$0.002 \le T \le 0.006$
	Anti-Vortex Plate Opening	Op (%)	$\%50 \le Op \le \%70$
	Blades Angle	θ (Degree)	$0 \le \theta \le 20$

In the table: Froude and Reynolds numbers are defined as $Fr = V/\sqrt{gD}$ and $Re = VD/\nu$ where ν is the kinematic viscosity of the fluid.

For flow discharge measurements, an electromagnetic flow meter (MAGFLO2500) with an accuracy of 1% installed in the path of the water return pipes into the reservoir was used (Fig. 5). To measure pressure fluctuations along the penstock, instantaneous pressure sensors were used (Fig. 6). Pressure fluctuations were measured in 9 sections at a distance of 0.5 meters from each other (Fig. 7). In addition, 4 piezometers in each section were embedded for measuring pressure fluctuations.

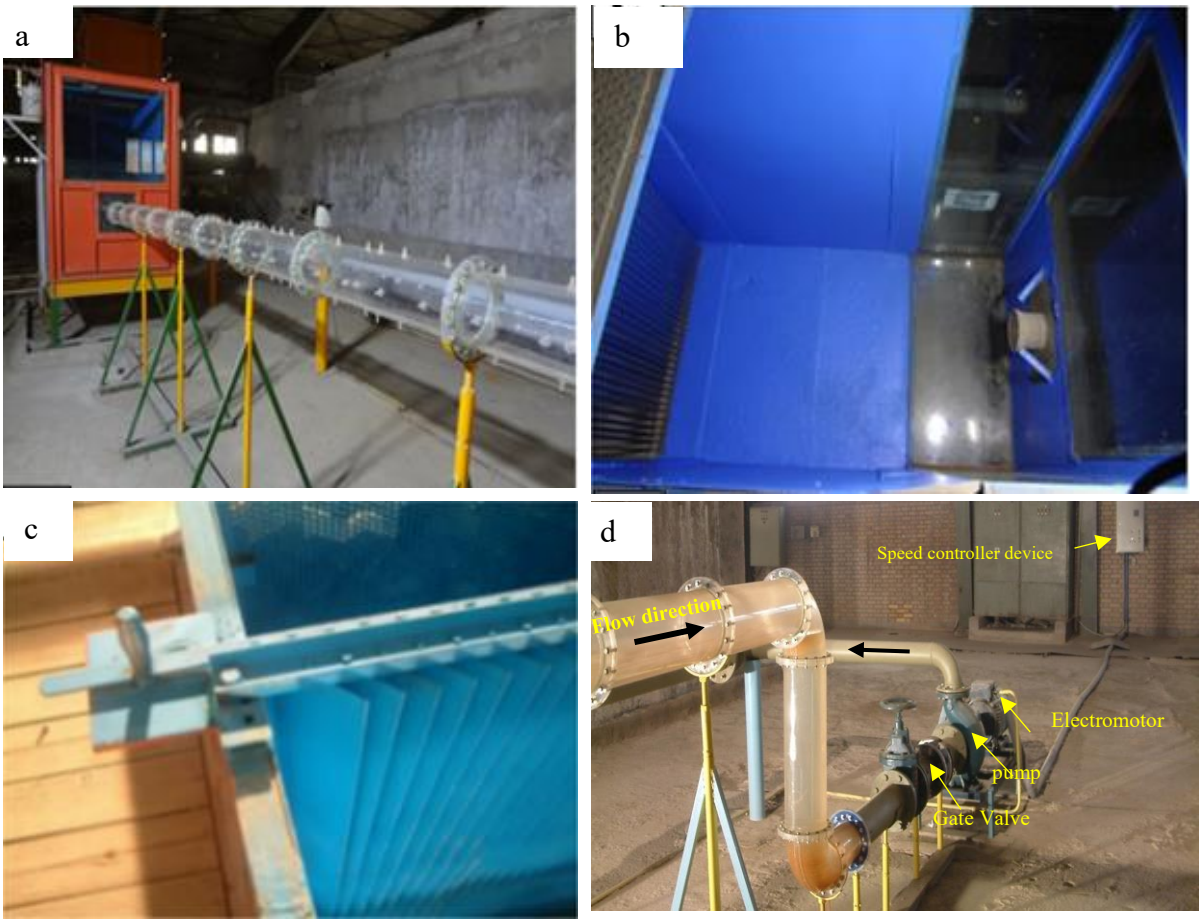

Figure 3. (a) Reservoir, transparent flow pipe; (b) glass walls of the reservoir and intake; (c) blades installed to create geometric asymmetry in model; (d) pump, electromotor speed controller device in laboratory model

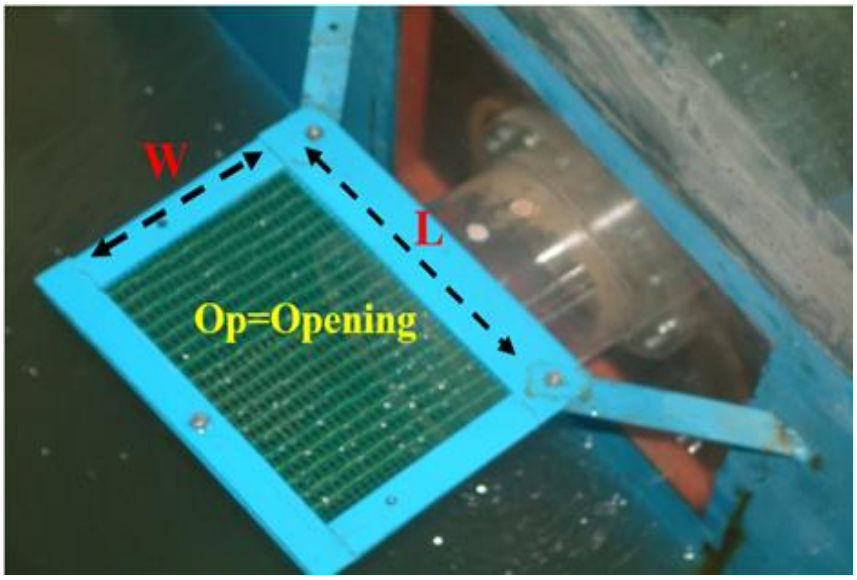

Figure 4. Perforated Horizontal plate installed on the forehead of the intake

Fig. 5. Flowmeter installed in the model

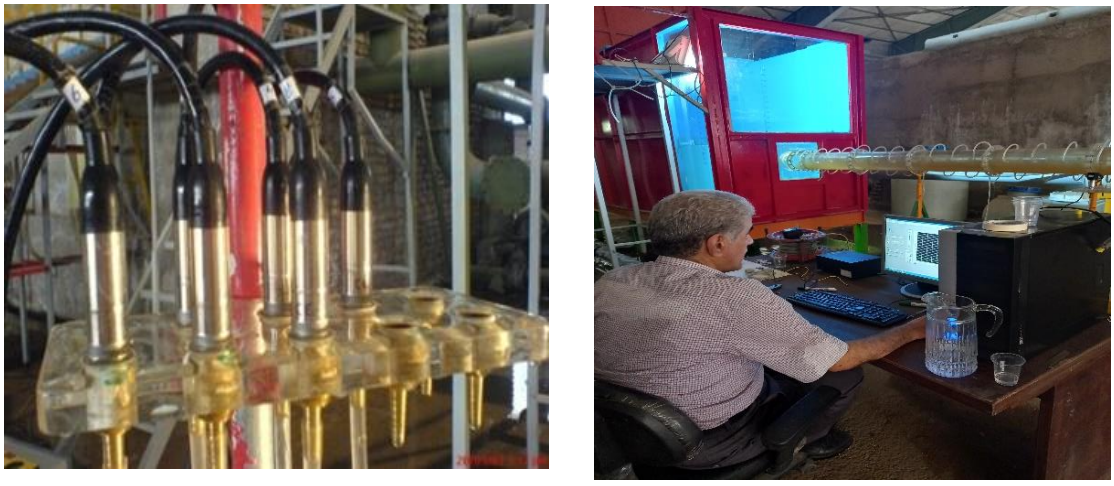

Figure 6. Instantaneous pressure sensors and dynamic pressure setup in the model

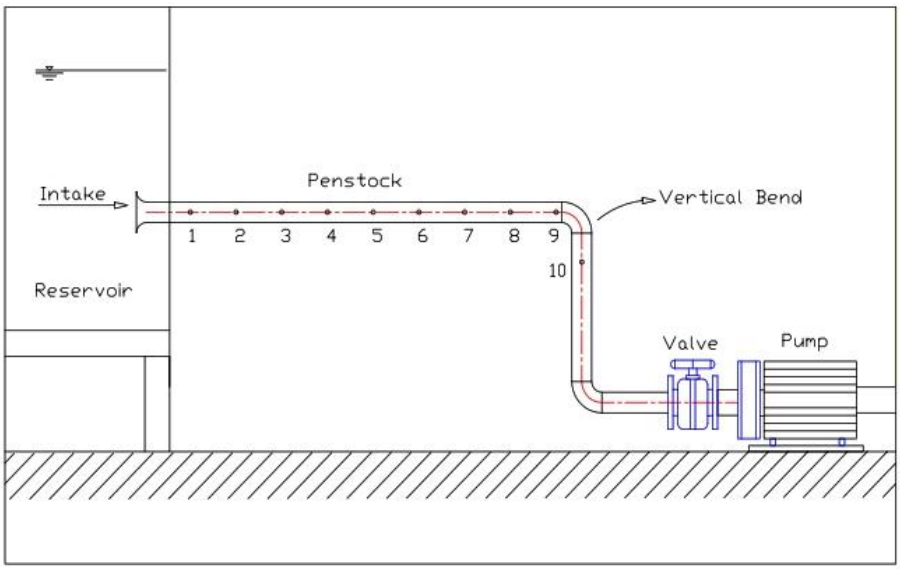

Figore 7. Dynamic pressure measurement sections along the penstock

Results

Effect of vortex on the head loss along the penstock

The experiments were carried out in the presence of the vortices with different classes. Five different relative submergence depths (S/D) in the reservoir as well as four Froude numbers (Fr) were considered. The selected range of Froude number and submergence depth includes all cases of the absence and the presence of possible weak and strong vortices at the intake. The values of the total head loss (ΔH) along the tunnel and relative total head loss (ΔH/H) are given in Table 2. To calculate the percentage of relative total head loss, the average pressure at section No.9 in Fig.7 was obtained and then the amount of the head loss was calculated from energy relationship between mentioned section and reservoir water surface and divide it by the reservoir head above the tunnel centerline (H or S).

The values in Table 2 indicate that at a certain relative submergence depth (S/D), with increase in Froude number, the amount of ΔH and ΔH/H have increased. The reason is that due to increasing the Froude number flow velocity in the Penstock increases and greater inlet and friction head loss in the presence of the anti-vortex plate is expected. In the condition without

the anti-vortex plate, in addition to the increase in the flow velocity in the Penstock, the increase in the order of the vortex by increasing Froude number is also another reason. For example, by increasing the Froude number from 0.6 to 1.2, the vortex order has increased from 2 to 6 (Roshan and Ghobadian, 2022). In other words, the area of the rotating flow inside the tank increases and vortex flow with the air core enters the Penstock, which has a higher energy loss.

Presence of the anti-vortex plate has caused the amount of energy loss to decrease in both absolute and relative forms. Values in tow last column of Table 2 identify that the reduction of ΔH/H due to the presence of the anti-vortex plate is between 1.4 to 6.1% for the reason that the anti-vortex plate plate at any relative submergence depth causes the order of the vortex to decrease or vortex be completely eliminated. In that case, the flow enters penstock with less disturbance and turbulence and as a result, the energy loss is less. Also, in general, with decrease in S/D, the amount of ΔH has increased, and effect of anti-vortex plate has become robust. The research of Roshan showed that with reduction of S/D, the size of the rotating area of the flow towards the Penstock intake increases (Roshan, 2023). In other words, the flow enters the Penstock with more turbulence, which increases the absolute energy loss. However, it is clear that with the increase in S/D, the relative head loss decrease, the main reason of that, is the increase of H (or S) in the denominator of the relative head loss relationship rather than the brief decrease of ΔH.

Table 2. Values of the total head loss(ΔH) and relative head loss (ΔH / H) along the tunnel in different (Fr) and (S/D)

S/D	Fr	Q (m3/s)	Average Press. Piz. 9 Without Plate (m)	Average Press. Piz. 9 With Plate (m)	ΔH (cm)		ΔH / H (%)	
					Without Plate (Strong Vortex)	With Plate	Without Plate (Strong Vortex)	With Plate
1.5	0.6	0.015	0.202	0.236	0.96	0.12	4.0	0.5
	0.8	0.020	0.171	0.233	1.87	0.65	7.8	2.7
	1.0	0.025	0.133	0.230	2.86	1.42	11.9	5.9
	1.2	0.030	0.087	0.226	3.96	2.54	16.5	10.6
1.75	0.6	0.015	0.240	0.277	1.12	0.05	4.0	0.2
	0.8	0.020	0.207	0.274	2.24	0.56	8.0	2.0
	1.0	0.025	0.179	0.271	2.83	1.18	10.1	4.2
	1.2	0.030	0.149	0.267	3.95	2.24	14.1	8.0
2	0.6	0.015	0.281	0.315	1.12	0.00	3.5	0.0
	0.8	0.020	0.251	0.313	1.86	0.38	5.8	1.2
	1.0	0.025	0.217	0.309	2.59	1.15	8.1	3.6
	1.2	0.030	0.198	0.304	3.71	1.82	11.6	5.7
2.5	0.6	0.015	0.364	0.393	0.76	0.00	1.9	0.0
	0.8	0.020	0.336	0.388	1.20	0.40	3.0	1.0
	1.0	0.025	0.305	0.377	1.84	1.24	4.6	3.1
	1.2	0.030	0.279	0.371	2.80	1.68	7.0	4.2
3	0.6	0.015	0.444	0.472	0.72	0.00	1.5	0.0
	0.8	0.020	0.420	0.463	1.10	0.43	2.3	0.9
	1.0	0.025	0.391	0.454	1.92	1.01	4.0	2.1
	1.2	0.030	0.370	0.444	2.83	1.82	5.9	3.8

Time (ms)

Fig. 8 shows the variations of the relative friction head loss(hf/L) in competition with Froude number in the absence and presence of anti-vortex plate. As it can be seen from Fig. 8, by increasing S/D, the amount of relative friction head loss (hf/L) increases. For a specific Froude number (constant velocity in the Penstock) with increasing values of S/D, the pressure inside the Penstock increases. Therefore, the fluid particles are in contact with each other and the tunnel wall with a higher pressure, so expect a greater friction loss. For example, in absence of anti-vortex plate, with the increase of the S/D from 1.5 to 3 at the highest Froude number, i.e. 1.2, the value of hf/L has changed from .75 to 1.35%. On the other hand, for the lowest Froude number, i.e. 0.6, with the increase S/D from 1.5 to 3, the relative friction loss has increased from .47% to .635%. On average, in the experiments of this research, by doubling the submergence depth, the amount of relative friction loss has increased by about 64%. Also, Fig. 8 shows for a certain S/D, increasing the Froude number increases the velocity of the flow in the tunnel and, as a result, increases the friction loss. Also, the effect of Froude number on the friction head loss is higher in the greater submergence depth. In general, in the condition of no anti-vortex plate, the Froude number increased from 6 to 1.2, the relative friction head loss increased from 0.57 to 1.05 %.

In addition, Fig. 8 indicate that the presence of the anti-vortex plate due to reduction of vortex effect has reduced the friction loss in the Penstock. The smaller S/D, the greater effect of the anti-vortex plate on the energy loss in the Penstock. The disturbance and turbulence of the flow inside the penstock due to the entry of the vortex with its air core can be the main reason for the increase in friction loss. Moreover, the possibility of the inversion of the flow velocity profile near the tunnel wall may increase the friction loss in the presence of a vortex. In this situation, in addition to steady friction loss, unsteady friction loss is also possible.

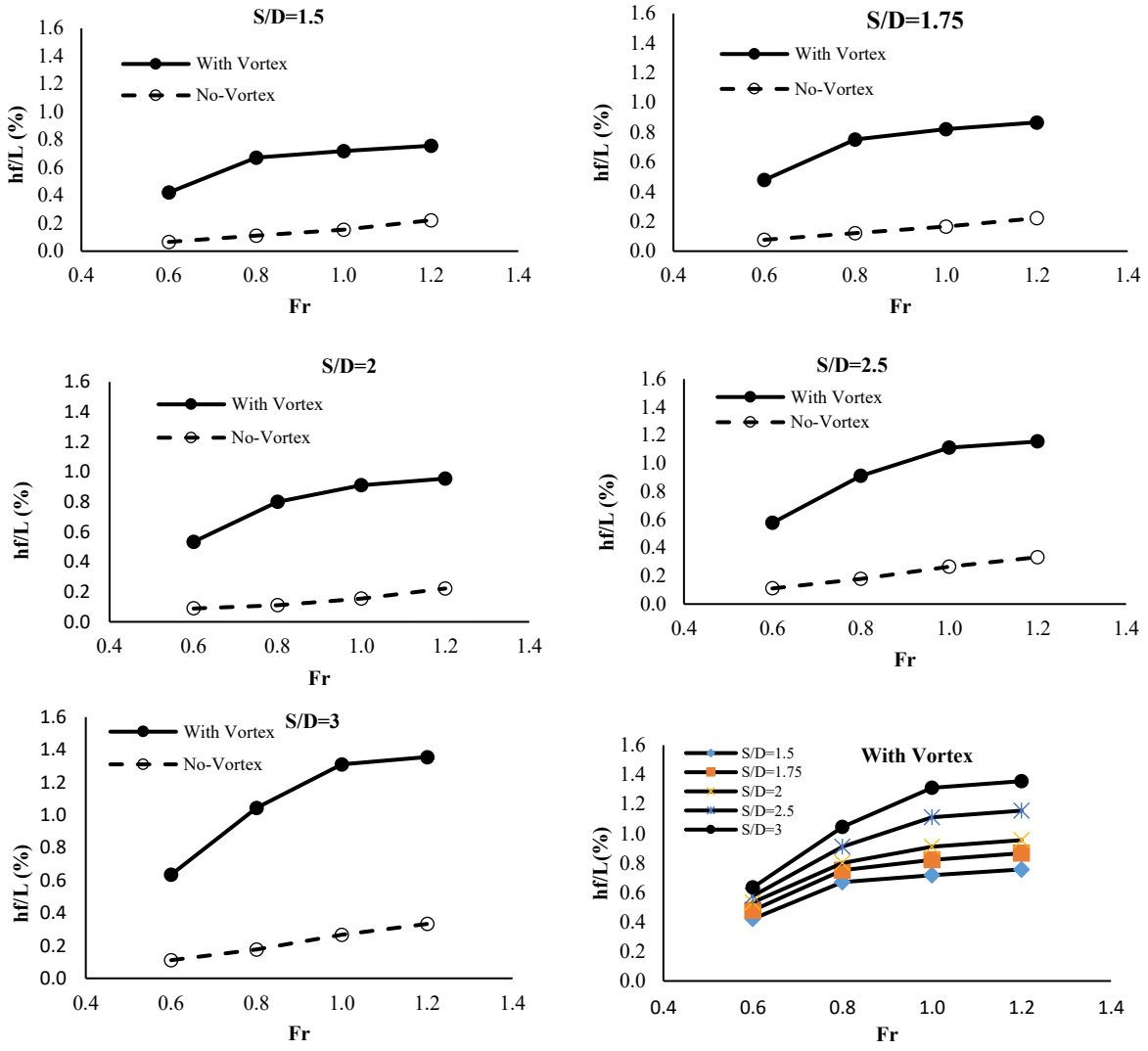

Figure 8. Variations of relative friction head loss vs. Froude number in different submergence depths with and without the presence of the vorticity control plate

Analysis of pressure fluctuations in the presence of vortices

Experiments in different conditions showed that even in the strongest air-core vortices, the swirling flows entering the tunnel concentrate near the tunnel crown. Therefore, among the four pressure sensors installed around each section of the tunnel, the sensor installed on the tunnel crown shows the most intense pressure fluctuations. For this reason, analyzes are presented only for the pressures recorded on the crown of the tunnel. In order to show the pressure fluctuating behavior of the flow along the penstock, the parameter of Fluctuating Intensity (FI) was defined as the following relationship:

$$FI=\frac{\sigma_P}{\bar{P}}=\frac{\sqrt{\frac{\sum_1^n (Pi-\bar{P})^2}{n}}}{\bar{P}} \quad (3)$$

Where standard deviation of the dynamic pressure data at each point is σ_P and $\bar{P}$ indicate the mean of the dynamic pressure data at the same point, Pi is each of value of measured

dynamic pressure data and n denote total number of observations. The closer the value of FE is to zero, it indicates less fluctuation in the flow and less deviation from the average pressure. Table 3 includes the absolute values of FI for different S/D and Fr along the tunnel. In this table (l) represents distance from beginning of tunnel and (L) is total length of the tunnel. The values presented in this table show that for the Froude number of 0.6, the maximum value of FI reaches about 2%. The reason for this low value is due to the formation of type 1or 2 vortex in this Froude number. While for the Froude number of 1.2 and the S/D of 1.5, which creates a vortex of order 6 (Roshan & Ghobadian, 2022), the value of FI reaches about 12.9%. As mentioned before, in the 6 order vortex, a strong swirling flow enters intake with an air core, which causes strong turbulence flow in the penstock.

Table 3. The absolute values of FI for different S/D and Fr along the tunnel

l / L (%)	Fluctuation Intensity (FI) - F_r = 0.6				
	S/D = 1.5	S/D = 1.75	S/D = 2	S/D = 2.5	S/D = 3
5	1.00	0.30	0.75	0.60	0.20
10	0.90	0.51	0.65	0.65	0.30
20	0.81	0.75	0.60	0.70	0.52
30	0.68	0.61	0.65	0.68	0.45
40	0.90	0.63	0.81	0.70	0.50
50	1.50	1.15	1.35	0.90	0.62
60	1.65	1.25	1.40	1.00	0.75
70	1.38	1.30	1.25	1.10	0.80
80	2.00	1.60	1.60	1.35	1.00
l / L (%)	Fluctuation Intensity (FI) - F_r = 0.8				
	S/D = 1.5	S/D = 1.75	S/D = 2	S/D = 2.5	S/D = 3
5	1.40	0.65	0.80	0.45	0.30
10	1.55	0.90	0.90	0.55	0.44
20	1.65	1.45	1.10	1.00	0.85
30	1.80	1.55	1.25	1.35	1.10
40	2.10	1.80	1.50	1.65	1.20
50	2.40	2.10	2.15	1.60	1.30
60	3.15	2.50	2.40	2.00	1.75
70	4.20	2.80	2.20	2.25	1.90
80	4.90	3.15	2.75	2.40	2.00
l / L (%)	Fluctuation Intensity (FI) - F_r = 1.0				
	S/D = 1.5	S/D = 1.75	S/D = 2	S/D = 2.5	S/D = 3
5	1.60	0.95	0.80	0.45	0.40
10	1.85	1.15	1.10	0.90	0.80
20	2.10	1.80	1.70	1.65	1.55
30	2.08	2.00	1.55	1.90	1.55
40	2.50	2.40	1.65	2.15	2.00
50	3.50	3.25	2.80	2.55	2.20
60	3.95	3.50	3.00	2.85	2.35
70	4.45	4.25	3.30	3.05	2.75
80	6.75	5.40	3.95	3.75	3.10
l / L (%)	Fluctuation Intensity (FI) - F_r = 1.2				
	S/D = 1.5	S/D = 1.75	S/D = 2	S/D = 2.5	S/D = 3
5	2.20	1.30	1.10	0.80	0.70
10	3.15	2.20	1.95	1.20	1.00
20	4.00	3.30	2.75	2.20	1.95
30	4.20	3.25	2.90	2.30	2.00
40	4.85	3.30	3.30	2.40	2.15
50	6.25	5.00	5.20	3.10	2.30
60	8.95	5.60	5.60	4.00	3.10
70	11.10	5.95	5.85	4.20	3.60
80	12.90	9.60	8.10	5.20	4.30

Fig. 9 shows variation of FI along Penstock. As it can be seen from this figure by increasing the distance from beginning of the penstock to the vertical bend, FI and in other words pressure fluctuations have also increased. This increasing trend can be seen for all relative submergence depths and all Froude numbers. However, this trend is greater at higher Froude numbers and smaller relative submergence depths. At higher Froude numbers and submergence depths, the 6 order vortex with the air core is formed and pulled into the water intake opening. When this strong swirling flow advances along the penstock, it moves across the flow to reach the crown of the tunnel and air bubbles are released inside the flow, causing more turbulence and fluctuations in the flow pressure. This issue was also seen through observations with dye injection. Fig. 10 shows a strong vortex with an air core stretching into the penstock in the model. As it can be seen from this figure, the vortex after entering the water intake, first moves downwards (to the vicinity of the tunnel axis) then it reaches the crown of the tunnel through a distance.

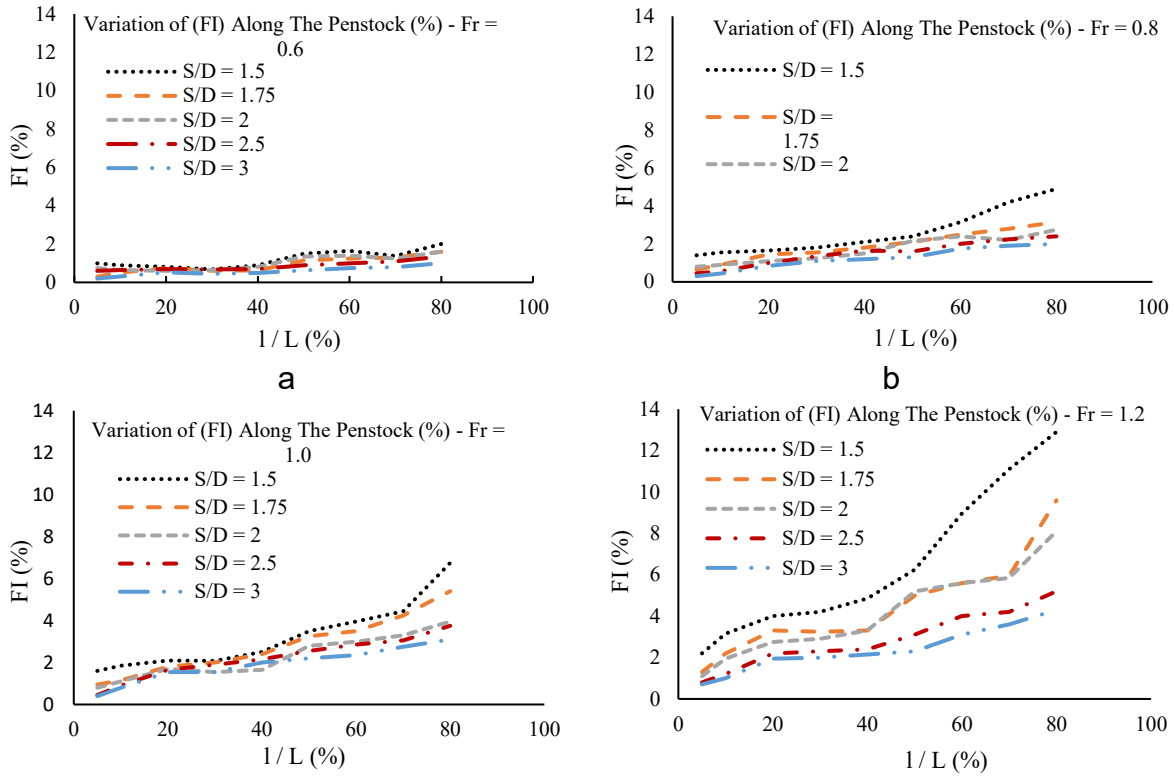

Figure 9. Variation of Fluctuating Intensity along the tunnel for (a) Fr = 0.6 , (b) Fr = 0.8 , (c) Fr = 1.0 and (d) Fr = 1.2

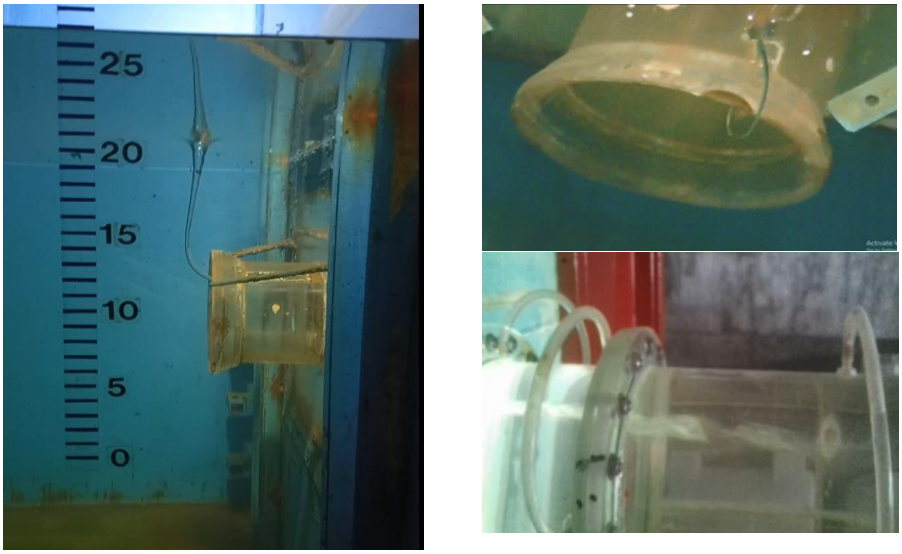

Figure 10. A strong vortex at the intake and the entry of swirling flow with an air core into the penstock

Vortex elimination along the Penstock

The vortex elimination trend was investigated along the tunnel for each of the three vortex groups shown in Fig 1. In order to achieve this goal, the pressure fluctuations were analyzed along Penstock, at any point where the trend of pressure fluctuations was fixed; it was introduced as the location of vortex elimination. In Fig 11, intensity of the pressure fluctuations (FI parameter represents the pressure fluctuation) is plotted against the relative length from the beginning of the Penstock. As shown in this figure, the type C weak vortex has eliminated in a length of about 25% or 7D from the beginning of the tunnel. For type B vortex, the effects of the vortex can be seen up to a relative distance of 65% or 18D from the beginning of the Penstock, and after that, the vortex is depreciated. In the case of strong air-core vortices, class A, by following the air core along the tunnel (as a parameter that shows the presence of the vortex) and reaching it to the bend, it seems that no length can be considered for vortex elimination. For this type of vortex, as shown in Fig 11, until the end of the penstock, which is about 30 times the diameter of the pipe, the pressure fluctuations have maintained their increasing trend. The reason for that is the growth of the flow rotation area and reaching to the inner wall of the pipe, that is, where the pressure sensors are installed.

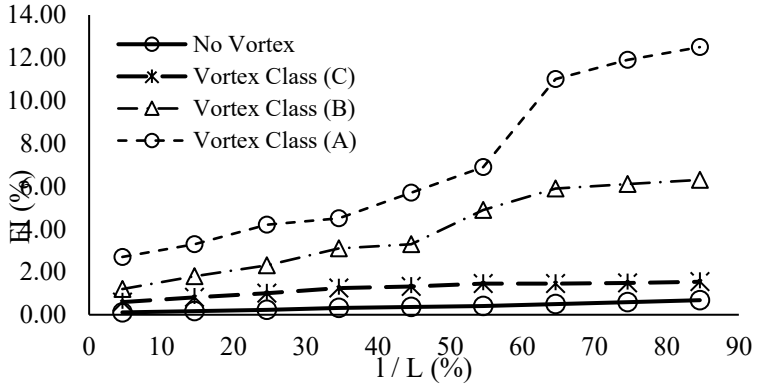

Figure 11. Fluctuating Intensity for different vortex classes along the tunnel

Friction coefficient in the penstock

The average values of the measured fluctuating pressures in piezometers No. 1 and 9 (Fig. 7) were determined to calculate head loss (h_f) along the Penstock. Values of friction coefficient (f) was determined for all experimental test using the Darcy-Weisbach equation ($h_f = f.\frac{L}{D}.\frac{V^2}{2g}$). Although the use of Darcy-Weisbach relationship is not completely suitable for the conditions of air in the pipe flow, nevertheless, due to the lack of an alternative relationship and its popularity, the aforementioned relationship was used. Variations of friction coefficient (f) against the Froude number for different relative submerged depths are presented in Fig 12.

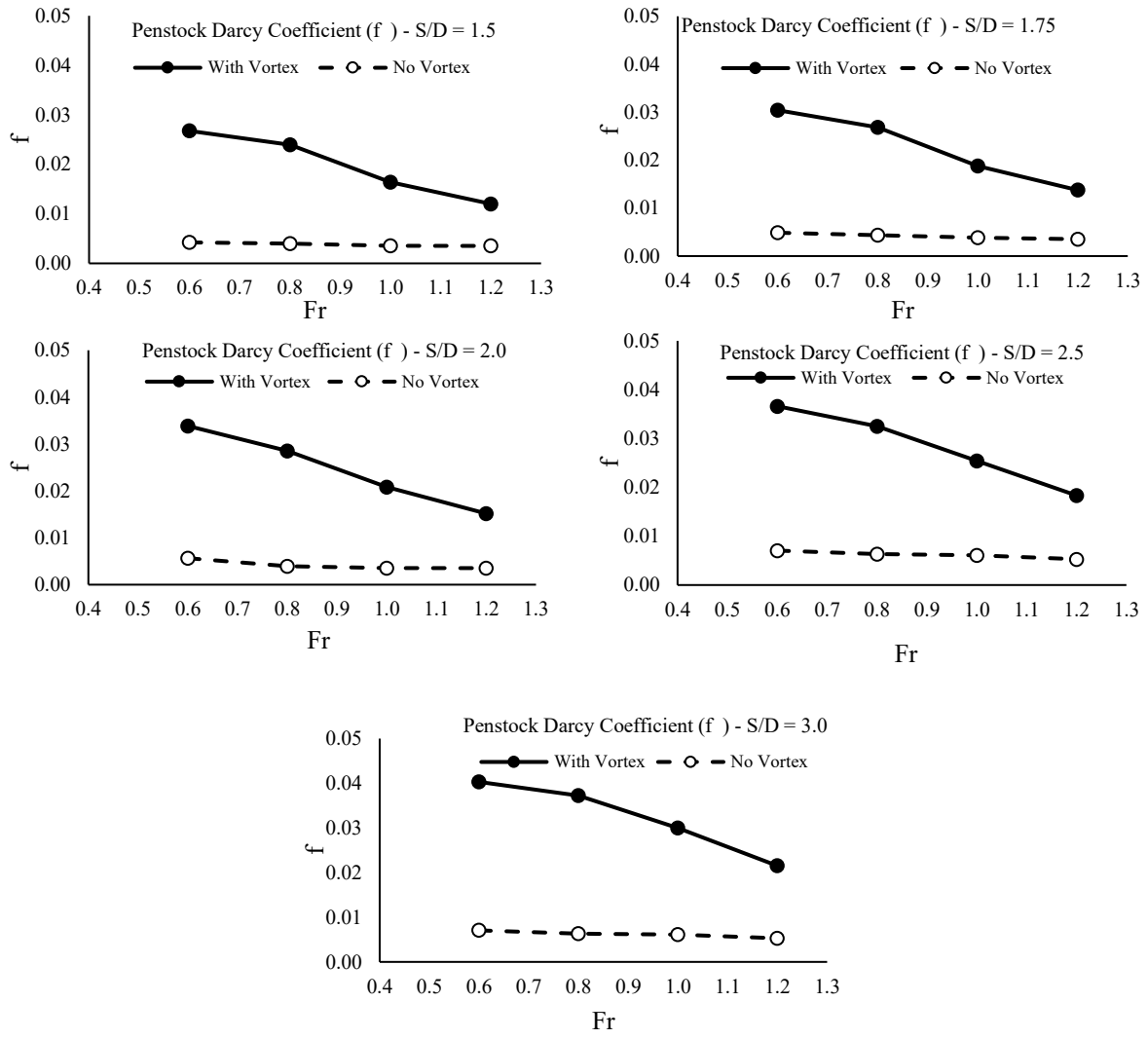

Figure 12. Variations of friction coefficient (f) against the Froude number for different relative submerged depths

As can be seen in Fig 12, for the condition that the anti-vortex plate is installed on the intake forehead, the formation of the vortex is prevented and the friction coefficient value are almost constant and is not affected by Froude number and submergence depth. Also, on average, the coefficient of friction loss in the state without vortex is 20% of this coefficient in the presence of a vortex, in other words vortex formation causes an increase in the friction coefficient in the tunnel. Furthermore, with the presence of the vortex, the largest values of the friction coefficient have been obtained at lower Fr and higher S/D. For example, in the Fr of 0.6 and the S/D of 3,

the presence of the vortex has increased the friction coefficient about 6 time in comparison with no vortex condition. On the other hand, by decreasing S/D and increasing Fr, where the strong vortices created, the lowest value of the friction coefficient has been obtained. The reason for this could be that increasing the Froude number increases the velocity of the flow in the penstock and makes the flow more turbulent, on the other hand, the decrease in the critical depth also causes the vortex to enter the penstock with a larger order, which also causes more turbulence in the flow. More turbulence means reducing the coefficient of friction loss, as in Moody's diagram, friction coefficient decreases with increasing flow velocity and Reynolds number. On the whole The results state that contribution of increasing Fr in reducing of friction coefficient is more than the reduction of the S/D.

Conclusions

The present study was conducted using a large-scale laboratory model. To date, no dedicated research has examined the influence of intake vortices on longitudinal head loss and friction coefficient in hydropower penstocks. Therefore, this investigation aimed to evaluate the effects of a wide range of vortex classes on head loss, friction coefficient, and pressure fluctuation intensity along the penstock through carefully controlled experiments.

The results demonstrated that the installation of an anti-vortex plate, designed to eliminate or reduce vortex strength, significantly decreased total energy loss in both absolute and relative terms. The relative total head loss reduction ($\Delta H/H$) achieved with the plate ranged from 1.4 % to 6.1 %. Furthermore, as the relative submergence ratio (S/D) decreased — corresponding to increased flow vorticity and enlargement of the rotating zone near the intake — the absolute head loss (ΔH) increased, and the beneficial effect of the anti-vortex plate became more pronounced.

For a constant Froude number, an increase in S/D led to higher internal pressure within the penstock and greater interaction between fluid particles and the tunnel wall, resulting in elevated relative friction loss (hf/L). In the presence of vortex flow, doubling the submergence depth increased the relative friction loss by approximately 64 % on average. Additionally, for a fixed S/D ratio, higher Froude numbers — associated with greater flow velocity — produced larger friction losses. The influence of the Froude number on friction head loss was found to be more significant at greater submergence depths.

On average, the friction coefficient (f) in vortex-free conditions was approximately 20 % lower than in the presence of vortices. Vortex formation consistently increased the friction coefficient within the penstock, with the highest values observed at lower Froude numbers and higher S/D ratios. Conditions that promoted higher-order vortices (potentially with an air-entraining core) — namely increased Froude number, reduced relative submergence, and removal of the anti-vortex plate — generated greater flow turbulence at the intake. As expected, the friction coefficient decreased with rising turbulence intensity.

Pressure fluctuation behavior along the penstock was analyzed by introducing the fluctuation intensity parameter FI (Equation 3). Strong vortices with an air core exhibited an increasing fluctuation trend between the intake and the downstream vertical bend. Weak Class C vortices dissipated within approximately 7D from the tunnel entrance, whereas the influence of Class B vortices persisted up to about 18D. No definite dissipation length could be established for strong Class A vortices within the tested tunnel length. Further experiments using substantially longer tunnels are recommended to determine the attenuation distance of high-strength vortices conclusively.

Author Contributions

All authors contributed to the study conception and design. Material preparation, data collection and analysis were performed by all authors.

Data Availability Statement

The data will be available upon reasonable request.

Acknowledgements

The model tests carried out at the Water Research Institute of the Ministry of Energy. In this way, the director and colleagues of the Hydraulic Structures Department of the Water Research Institute, especially Dr. Amir Reza Zarrati and Dr. Hamed Sarkardeh, are sincerely appreciated.

Ethical Considerations

The authors avoided data fabrication, falsification, plagiarism, and misconduct.

Funding

That no funds, grants, or other support were received during the preparation of this manuscript.

Conflict of Interest

The authors declare that they have no conflict of interest.

References

Agbayani, N., Karami, H., Mousavi, S.F., & Sarkardeh, H. (2019). Experimental study of the effect of the trashrack on the vortex at the intake of the hydroelectric power plants in various flow rates and submergence depths. *Journal of Dam and Hydroelectric Power plant*, 6(21),49-62. https://www.researchgate.net/publication/334770912_Experimental_study_of_the_effect_of_the_trashrack_on_the_vortex_at_the_intake_of_the_hydroelectric_power_plants

Amiri, S. M., Zarrati, A. R., Roshan, R., & Sarkardeh, H. (2011). Surface vortex prevention at power intakes by horizontal plates. *Journal of Water Management (ICE)*, 164(4),193-200. https://doi.org /10.1680/wama.1000009

Azarpira, M., Sarkardeh, H., Tavakkol, S., Roshan, R., & Bakhshi, H. (2014). Vortices in dam reservoir: A case study of Karun III dam. *Journal of Sādhanā*, 39(5), 1201-1209. https://doi.org/10.1007/s12046-014-0252-7

Bajracharya, T. R., Shakya, S. R., Timilsina, A. B., & Dhaka, J. (2020). Effects of geometrical parameters in gravitational water vortex turbines with conical basin. *Journal of Renewable Energy*. 1-16. https://doi.org/10.1155/2020/5373784

ÇELEBIOĞLU, K. (2019). Roughness coefficient of a highly calcined penstock. *Teknik Dergi, Paper 545*, 9309-9325. https://doi.org/10.18400/tekderg.447265

Constantinescu, G. S., Patel, V. C., 1998, A numerical model for simulation of pump intake flow and vortices. *Journal of Hydraulic Engineering*, 124(5), 123-134. https://doi.org/10.1061/(ASCE)0733-9429(1998)124:2(123)

Daggett, L. L.,& Keulegan, G. H. (1974). Similitude in free-surface vortex formation. J Hydraul Eng, 100, 1565–1580. https://doi.org/10.1061/ JYCEAJ.0004105

Guilliver, J.S., & Rindels, A. J. (1987). Weak vortices at vertical intakes. *Journal of Hydraulic Engineering*, 113(9), 1101-1116. https://doi.org/10.1061/(ASCE)0733-9429(1987)113:9(1101)

Jain, A. K., Raju, K. G. R., & Garde, R. J. (1978). Vortex formation at vertical pipe intake. *J Hydraul Eng* , 100(10), 1427–1445. https://doi.org/ 10.1061/JYCEAJ.0005087

Keller, J., Möller, G., Boes, R.M. (2014). PIV measurements of air-core intake vortices. *Journal of Flow Measurement and Instrumentation*, 40(40), 74–81. https://doi.org/10.1016/j.flowmeasinst.2014.08.004

Leon, A. S. (2016). Determining optimal discharge and optimal penstock diameter in water turbines, international symposium on hydraulic structures. *Utah State University*, Portland, Oregon, USA, 27-30. https://doi.org/10.15142/T390628160853

Manogaran, T., Zainol, M. R. R. M. A., Wahab, M. K. A., Aziz, M. S. A., Abd Aziz, N., Zahari, N. M., & Radzi, M. R. M. (2023). Free-surface vortices mitigation using anti-vortex plates in dam intakes through CFD. *CFD Letters*, 15(6), 26-41. https://doi.org/10.37934/cfdl.15.6.2641

Möller, G. Detert, M., & Boes, R. M. (2015). Vortex-induced air entrainment rates at intakes, *Journal of Hydraulic Engineering*, 141(11), 1-8. https://doi.org/10.1061/(ASCE)HY.1943-7900.0001036

Möller, G., Detert, M., & Boes, R. M. (2012). Air entrainment due to vortices: State-of the-art. 2nd International Association of Hydraulic Engineering Europe Congress, *IAHR Press*, Munich, Germany. http://hdl.handle.net/20.500.11850/63100

Moukam, T., François, N., Thomas, D., & Bienvenu, K. (2022). Numerical evaluation of turbulent friction on walls in the penstock of the Three-Gorges Dam by the Swamee-Jain method. *International Journal of Civil and Environmental Engineering*, 16(6). https://doi.org/10.2166/nh.2024.054

Odgaard, A. J. (1986.) Free surface air core vortex. *J Hydraul Eng* , 112(7), 610–619. https:// doi. org/ 10. 1061/(ASCE) 0733- 9429(1986)112:7(610)

Padmanabhan, M., & Larsen, J. (2001). Chapter 10.2: Intake modeling. Pump handbook, *McGraw-Hill*, New York. https://turbosan.com/pdf/pumphandbook.pdf

Partovi Azar, S. , Farsadizadeh, D. , Hosseinzadeh Dalir, A. , Salmasi, F., & Sadraddini, A. (2010). Estimation of Critical Submergence at Intake System of Aydoghmush Dam Using FLUENT Model. *Water and Soil Science*, *20*(3), 1-14. https://water-soil.tabrizu.ac.ir/article_1328.html?lang=en

Rahm, L. (1953). Flow problems with respect to intakes and tunnels of Swedish hydro-electric power plants. Bulletin, No. 36, *Institution of hydraulic at the Royal Institute of Technology*, Stockholm, Sweden. https://public.ucrlib.aspace.cdlib.org/repositories/5/archival_objects/582280

Roshan, R. (2023). Laboratory investigation on the effect of anti-vortex plates and reservoir geometry on the hydrodynamics of vortex flow in power plant Intakes. PhD thesis in hydraulic structures, *Razi University*, Kermanshah, Iran.

Roshan, R., & Ghobadian, R. (2022). The Effect of anti-vortex plates on vortex dissipation, discharge coefficient and inlet loss coefficient in hydropower intakes. *Journal of Hydraulics*, 17(3), 15-29. https://doi.org/10.30482/jhyd.2022.302255.1547

Roshan, R., & Ghobadian, R. (2023). The effect of reservoir geometry on the critical submergence depth in hydroelectric power plants intake. *Applied Water Science*, 13, 155, 2-9, https://doi.org/10.1007/s13201-023-01960-z

Sarkardeh, H., Jabbari, E., Zarrati, A.R., & Tavakkol, S. (2013). Velocity field in a reservoir in the presence of an air-core vortex. *Journal of Water Management (ICE)*, 164(4), 193–200. https://doi.org/ 10.1680/wama.13.00046

Sarkardeh, H., Zarrati, A. R., Jabbari, E., & Roshan, R. (2012). Discussion of prediction of intake vortex risk by nearest neighbors modeling. *Journal of Hydraulic Engineering*, 137(6), 701-705. https://doi.org/10.1061/(ASCE)HY.1943-7900.0000344

Sarkardeh, H., Zarrati, A. R., & Roshan, R. (2010). Effect of intake head wall and trash rack on vortices. *Journal of Hydraulic Research*, 48(1), 108-112. https://doi.org/10.1080/00221680903565952

Singhal, M. K., & Kumar, A. (2015). Optimum design of penstock for hydro projects. *International Journal of Energy and Power Engineering* , 4(4), 216-226. https://doi.org/10.11648/j.ijepe.20150404.14

Suerich-Gulick, F., Gaskin, S. J., Villeneuve, M., & Parkinson, É. (2014). Characteristics of free surface vortices at low-head hydropower intakes. *Journal of Hydraulic Engineering*, 140(2), 291-299. https:// doi.org /10.1061/(ASCE)HY.1943-7900.0000826

Sukhapure, K., Burns, A., Mahmud, T., & Spooner, J. (2018). CFD modelling and validation of loss Coefficients for penstock bifurcation in hydropower schemes. *3rd Thermal and Fluids Engineering Conference (TFEC)*, 395-406.http://dx.doi.org/10.1615/TFEC2018.cmd.021574

Zheng, G., Gu, Z., Xu, W., Lu, B., Li, Q., Tan, Y., & Li, L. (2023). Gravitational surface vortex formation and suppression control: A review from hydrodynamic characteristics. *Processes*, 11(42), 3-20. https://doi.org/10.3390/pr11010042